

Designing and 3D printing continuous fibre-reinforced composites with a high fracture toughness

Yentl Swolfs^{1,2}, Silvestre Pinho²

¹Department of Materials Engineering, KU Leuven, Kasteelpark Arenberg 44, B-3001 Leuven, Belgium.

²Department of Aeronautics, Imperial College London, South Kensington Campus, SW7 2AZ, London, United Kingdom.

ABSTRACT

The translaminar fracture toughness determines in many cases the damage tolerance of composite components, and this property is strongly influenced by the microstructure. A finite element model was developed that can aid in the optimisation of the microstructure for maximising the translaminar fracture toughness of composites hybridised at the tow level. The model proved that the toughness is increased when the crack has to grow through an interface between carbon and glass in a hybrid composite. This implies that the microstructure can be optimized to maximize the translaminar fracture toughness. Hybridisation at the tow level is now possible by using micro-tow placement machines. Therefore, samples were 3D-printed with continuous fibres. Therefore, samples were 3D printed with continuous fibres. Compact tension tests indicated that the toughness can indeed be increased by fibre-hybridization. This provides new avenues for improving the damage tolerance of composite materials.

INTRODUCTION

Conventional manufacturing processes create significant waste and left-overs. 3D printing however creates near-net shape components and allows materials usage of well over 90%. This leads to a more environmentally friendly production process. Additionally, it also does not require an expensive mould and allows to create more complex parts that can easily be custom-made. Traditionally, 3D printers have focused on metals and polymers, and the field of fibre-reinforced composite 3D printing has been relatively narrow. Most attempts so far have focused on discontinuous fibre-reinforced composites [1]. The discontinuous nature leads to reductions in alignment and less efficient load transfer. This limits the stiffness and strength improvements over unreinforced plastics.

Much greater improvements can be achieved with continuous fibres, but laying down small bundles of continuous fibres also more challenging from a processing view. Recently, the first 3D printer for continuous fibre-reinforced composites came onto the market. This printer puts down individual impregnated tows in each layer, and builds up the composite layer-by-layer. The process can therefore also be called 2.5D printing or micro-tow placement.

By laying down individual tows, the printer allows great versatility in designing microstructures that are difficult, if not impossible, to achieve with conventional composite manufacturing processes. The microstructure is often crucial for the mechanical performance of composites, and 3D printing hence offers scope for improved mechanical performance. One such property is the translaminar fracture toughness, for which it is well recognised that the microstructure plays a key role. When this microstructure is engineered, large improvements in toughness are possible [2, 3].

Another way to improve the mechanical properties beyond expectations is through fibre-hybridisation [4]. By combining two fibre types in the same matrix, it becomes possible to achieve synergetic effects. The literature on hybrid composites offers many examples of

synergetic effect for a variety of mechanical properties [5]. For translamellar fracture toughness however, no studies have been published.

The focus here lies on improving the translamellar fracture toughness of continuous fibre-reinforced composites by optimising the microstructure. A finite element model for predicting the optimal microstructure of carbon/glass hybrid composites will be developed and experimentally validated.

FINITE ELEMENT MODEL

Description of the model

The finite element model is developed in Abaqus/Explicit. To allow the model to predict complex microstructures, a 3D model is needed within the fracturing region. Outside the fracture region however, the composite can be represented by 3D shell elements, which significantly reduces the computational cost (see Figure 1). The solid region is composed of hexahedral, reduced integration elements except for the first layer of elements in the fracturing region, which was composed of full-integration elements to avoid hourglassing. Outside the fracturing region, the microstructure does not need to be explicitly represented by solid elements. These elements were therefore replaced by shell elements. The shell regions consisted of quadrilateral shell elements with reduced integration. This combination yielded a good accuracy at a limited computational cost.

The model (see Figure 1) is 60 mm high, 65 mm long and 1 mm thick. The solid region is 4 mm high, 50mm long and 1 mm thick. A displacement boundary condition is applied at 16 mm from the symmetry plane and 14 mm from the left-hand side. A relative displacement of 8 mm is applied over a total time of 0.1s using a smooth ramp-up in the beginning to avoid any unwanted stress waves. The initial notch is 19 mm long.

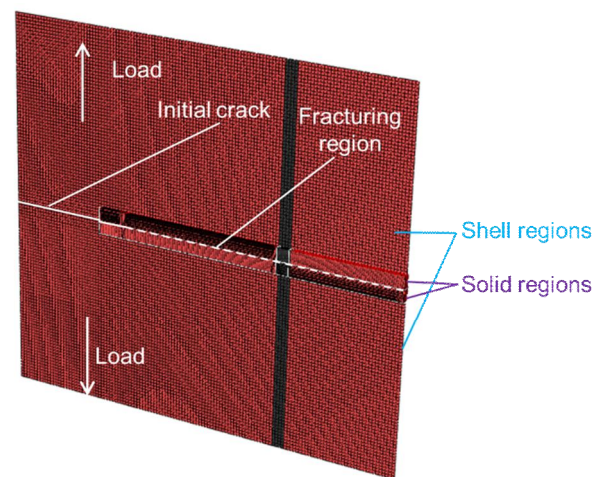


Figure 1. The finite element model with indication of the shell and solid regions.

Two sets of material properties were used in the models (see Table I). These properties are reasonable values for a balanced 0/90 layup of 3D printed carbon fibre/nylon and glass fibre/nylon. All interfaces between carbon and glass fibre composites are separated by a layer of cohesive elements. These cohesive elements cannot break and prevent computational problems

due to nodes being linked to two distinct cohesive surfaces. The elements are only 10 μm and do not influence the modelling results.

Six different models were created (see

Figure 2). These models are labelled using GF for glass fibre composites and CF for carbon fibre composites. The order of the labelling systems corresponds to the order in which the crack grows through the two materials. For example, the crack in $\delta\text{GF-CF}\delta$ starts off in the glass fibre composite, and then grows into the carbon fibre composite.

The displacement was applied over a total time step of 0.1s, using a smooth amplitude to ramp up the displacement in the beginning. A mass scaling of 40 times was applied to the cohesive elements to ensure that they did not limit the stable time increment. The other elements were not mass scaled. The linear and quadratic bulk viscosity were set to 0.02 and 0.4.

TABLE I. Engineering constants and translaminar fracture toughness parameters for carbon and glass fibre/epoxy composites.

	E_1 (GPa)	E_2 (GPa)	E_3 (GPa)	G_{12} (GPa)	G_{13} (GPa)	G_{23} (GPa)	G_{12} (GPa)	G_{13} (GPa)	G_{23} (GPa)	G_{Ic} (kJ/m ²)	G_{IIc} (MPa)
Carbon fibre composite	37.5	37.5	1.0	0.010	0.352	0.352	3.7	3.7	3.7	125	1000
Glass fibre composite	13.9	13.9	1.0	0.026	0.341	0.341	3.7	3.7	3.7	250	500

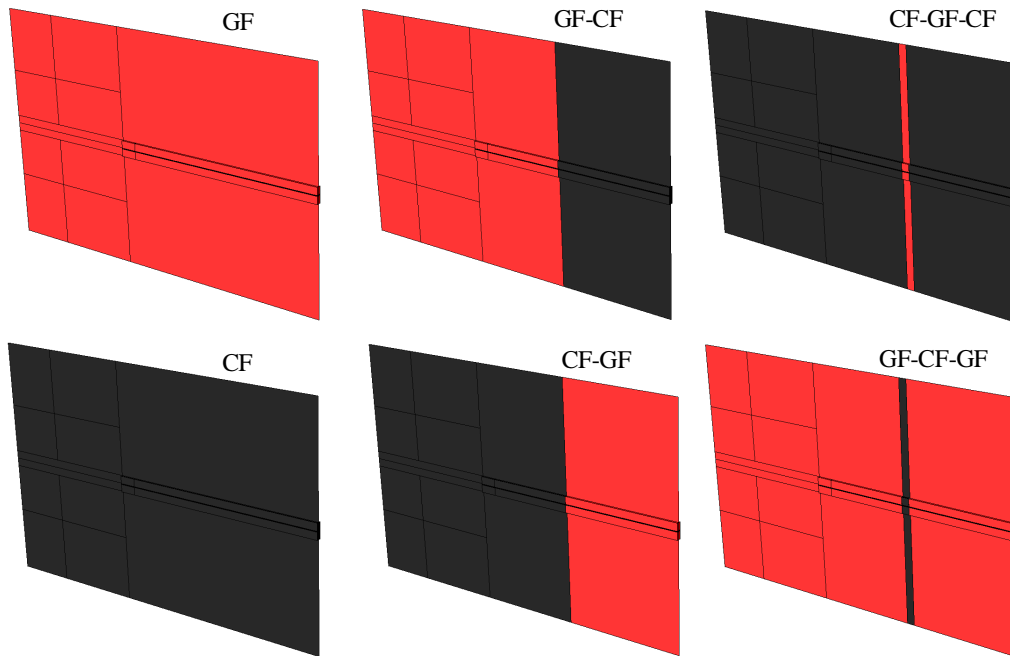


Figure 2. 3D view of the six different models, with red indicating glass fibre composites and dark gray indicating carbon fibre composites.

The kinetic energy was always less than 5% of the strain energy to ensure that the model can be considered quasi-static. Load oscillations were however inevitable during unstable crack growth, and further damping was provided by dashpots. These dashpots were placed at strategic locations near interfaces between carbon and glass fibre layers. The fracture toughness at any

given time was calculated by locally measuring the crack opening displacement and traction, and integrating the resulting diagram.

Results

Figure 3 presents the load-displacement diagrams of the six models shown in

Figure 2. As expected, the two reference composites $\delta GF\ddot{o}$ and $\delta CF\ddot{o}$ reveal a decreasing load as the crack grows. The load does oscillate slightly, which is linked to energy being released when the crack grows.

An interesting feature is observed for $\delta GF-CF-GF$ and $\delta GF-CF\ddot{o}$ composites. The decrease that was seen for the reference composites is now converted into a plateau with a small increase at the end. This indicates that it is difficult for a crack to grow from a glass fibre composite into a carbon fibre composite. Growing through this interface takes up so much energy that the two halves of the models dislodge completely after the crack passes the interface.

A similar plateau is not found for the $\delta CF-GF\ddot{o}$ and $\delta CF-GF-CF\ddot{o}$ hybrids. This implies that growing a crack from a carbon fibre composite into a glass fibre composite is comparatively less challenging. The sudden change in stiffness around the crack tip does cause variations in the load.

The toughness for the GF and CF composite reveals a uniform value after the initial build-up region. The most interesting feature again arises for the GF-CF-GF and GF-CF hybrids. These models reach fracture toughness values of up to 110 kJ/m², which is higher than either of the constituent properties. This is hence a true synergetic effect.

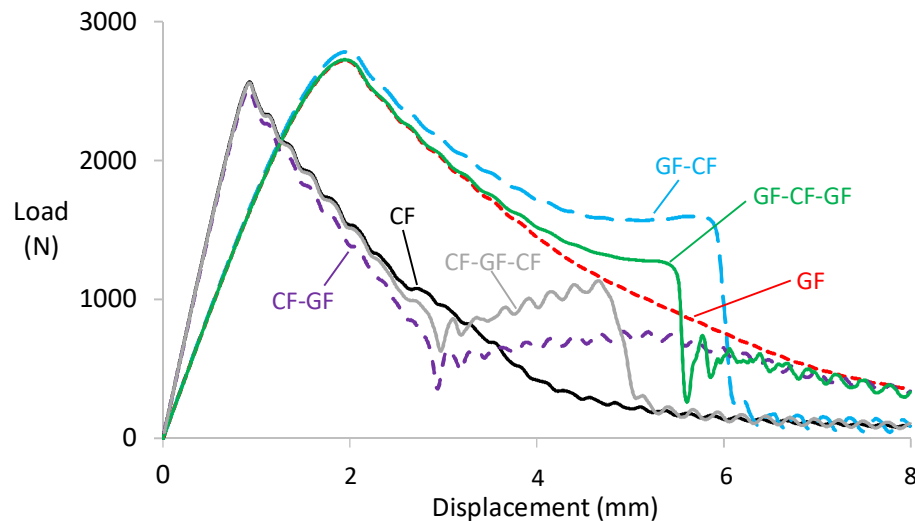


Figure 3. Load-displacement diagram for the six models.

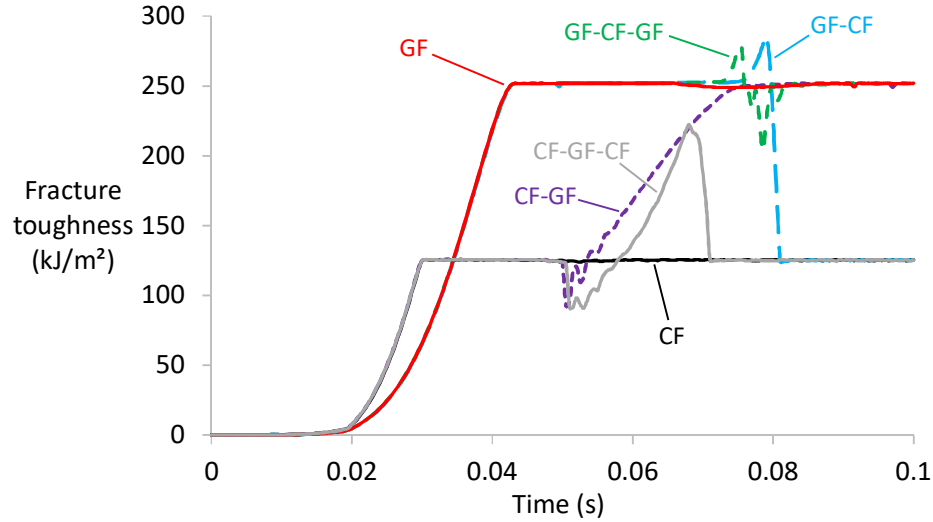


Figure 4. The toughness evolution as a function of the time, revealing a synergetic effect for the GF-CF-GF and GF-CF composites.

EXPERIMENTS

Materials and 3D printing

Nylon, carbon fibre/nylon and glass fibre/nylon spools were sourced from MarkForged, and used on a MarkOne printer. The nylon is a blended grade with an undisclosed composition. All layer thicknesses were 100 μm . The tensile modulus was measured to be 0.45 GPa. The fibre volume fraction of the fibre-reinforced spools was measured to be 31%.

The compact tension samples were printed in two steps. Firstly, a rectangular specimen was printed with a central, 3.8 mm thick core of fully unidirectional material. While the unidirectional core can be either glass fibre/nylon or carbon fibre/nylon, the outer 0.6mm on either side always consisted of pure nylon. This 0° specimen is then overprinted with 90° fibres. The overprinting is needed to get 90° fibres in the specimen, which helps to avoid unwanted failure mechanisms during the compact tension test. The overprinting added 800 μm of 90° glass fibre layers on either side of specimen.

A total of four specimens were successfully printed and tested. Three of these specimens were non-hybrid glass fibre composites. The fourth one was a hybrid composite, where the central 0° ply contained a strip of 1 mm thick carbon fibre ply.

Testing methodology

As is usually the case with 3D printed samples, the bonding between the layers is relatively weak. This made compact tension tests challenging to perform. Several approaches were combined to achieve a successful failure during compact tension. Firstly, the double-tapered specimen design from Blanco et al. [6] was water jet cut into the specimens to reduce compressive forces. Secondly, the initial notch was machined to be 25 mm long. Thirdly, inspired by the metals standard for compact tension, an edge groove was machined by a rotating blade. This blade had a diameter of 50 mm and a thickness of 0.8 mm. The edge groove was machined on either side to leave about 800 μm of the 0° ply in the middle. The edge groove did not run all the way to the back of specimen, but was stopped 5mm before the end. This ensures that there is sufficient material left to resist the compressive forces.

Finally, two anti-buckling guides were added to prevent buckling at the back of the specimen. These guides were held together by two M8 bolts, which were tightened by hand. This still allowed relative sliding, and it was verified that the guide did not affect the load measurements.

A machine displacement rate of 1.25 mm/min was applied. The displacement near the loading holes was measured optically. The data reduction was done using the compliance calibration method. The plasticity of the nylon matrix prevent a good fit with the optical observation of the crack growth. The compliance calibration data was therefore scaled to fit the experimental crack growth versus compliance diagram.

Results

The R-curves for the four tested samples are shown in Figure 5. Two of the glass fibre curves reveal a translaminal fracture toughness of around 250 kJ/m², while the third one is significantly tougher. This is likely to be due to inherent variations in the bonding of the printed bundles. This difference is also seen on the fracture surfaces, with the tougher samples having much longer fibre pull-out lengths.

The most interesting behaviour in the R-curve is however that of the hybrid composite. When the crack tip approaches the carbon fibre strip, the fracture toughness shows a distinct increase. This confirms the modelling result that it is difficult for a crack to grow through a glass/carbon interface. This promising finding can now be exploited to further optimise the microstructure.

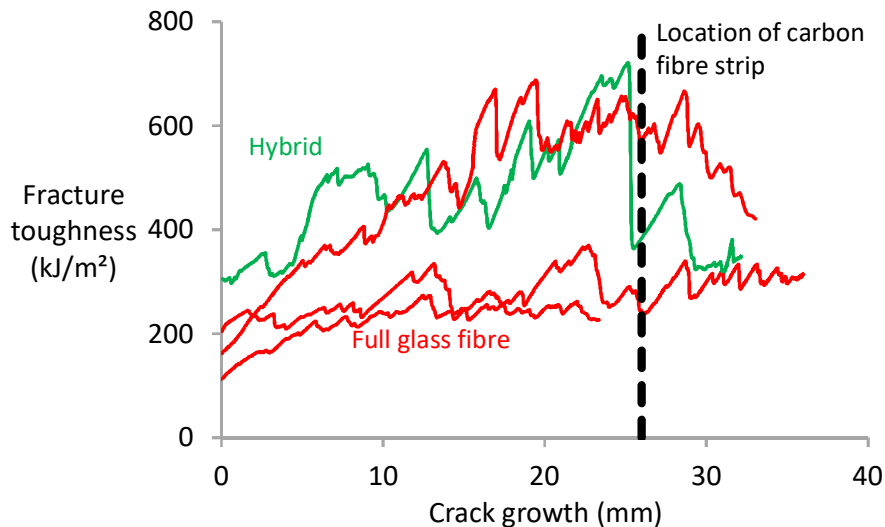


Figure 5. The R-curves reveal that the resistance to crack growth of the hybrid composite increases when the crack approaches the carbon fibre strip.

CONCLUSION

A finite element model was developed that can aid in the optimisation of the microstructure for improving the translaminal fracture toughness. The model revealed that growing a crack from a glass fibre composite into a carbon fibre composite is associated with an increased toughness. This finding was experimentally validated using 3D printed hybrid composites, which revealed a marked toughness increase before crack growth through the interface. In the future, this model will be used to predict the optimal microstructure and to perform a parametric study

on the optimal parameters for maximising the synergetic effect. The optimised microstructures will then be tested experimentally.

ACKNOWLEDGMENTS

The authors acknowledge the support of the European Commission for the Marie Skłodowska-Curie Individual European Fellowship "HierTough" for YS. YS acknowledges the support of FWO Flanders for his postdoctoral fellowship. STP acknowledges EPSRC for his fellowship under grant EP/M002500/1.

REFERENCES

1. Quan, Z., A. Wu, M. Keefe, X. Qin, J. Yu, J. Suhr, et al. 2015. "Additive manufacturing of multi-directional preforms for composites: opportunities and challenges," *Mater. Today*, 18(9):503-512.
2. Bullegas, G., S. T. Pinho, and S. Pimenta. "Engineering the translaminar fracture behaviour of thin-ply composites," *Compos. Sci. Technol.*, 131:110-122.
3. Laffan, M. J., S. T. Pinho, P. Robinson, and L. Iannucci. 2010. "Measurement of the in situ ply fracture toughness associated with mode I fibre tensile failure in FRP. Part II: Size and lay-up effects," *Compos. Sci. Technol.*, 70(4):614-621.
4. Swolfs, Y., L. Gorbatikh, and I. Verpoest. 2014. "Fibre hybridisation in polymer composites: a review," *Compos. Part A: Appl. Sci.*, 67:181-200.
5. Swolfs, Y., R. M. McMeeking, L. Gorbatikh, and I. Verpoest. 2015. "The effect of fibre dispersion on initial failure strain and cluster development in unidirectional carbon/glass hybrid composites," *Compos. Part A: Appl. Sci.*, 69:279-287.
6. Blanco, N., D. Trias, S. T. Pinho, and P. Robinson. 2014. "Intralaminar fracture toughness characterisation of woven composite laminates. Part I: Design and analysis of a compact tension (CT) specimen," *Eng. Fract. Mech.*, 131:349-360.